MEASUREMENT OF THE VIBROACOUSTIC INDICATORS OF SANDWICH COMPOSITE STRUCTURES

A. Raef Cherif[1], B. Noureddine Atalla[1*] and C. Andrew Wareing[2]
[1]GAUS
University of Sherbrooke, Sherbrooke (Québec), CANADA
Email: Raef.Cherif@usherbrooke.ca, Noureddine.Atalla@usherbrooke.ca

[2] Bombardier Aerospace,
123 Garratt Blvd, North York M3K 1Y5, Ontario, CANADA
Email: Andrew.Wareing@aero.bombardier.com

ABSTRACT

This paper discusses the measurement of the vibroacoustic indicators of two sandwich-composite structures over a large frequency band. Several indicators are investigated including the structural wavenumber, modal density, damping loss factor, radiation efficiency, and sound transmission loss. For the first four indicators several direct and indirect measurements techniques are presented and compared. Moreover, the measured indicators are compared to analytical predictions. Results show that all measured indicators are in good agreement with theory for the studied constructions.

1 INTRODUCTION

Composite sandwich panels are used in several applications due to their favorable stiffness to weight ratios. Such panels are composed of thin composite face sheets and a shearing core. Unfortunately, these panels do not provide suitable sound insulation or good vibration damping characteristics. Indeed, they may depict a wide area of acoustic coincidence, starting at low frequencies, leading to increased radiation efficiency, which can lead in some instances to higher interior noise levels [1]. Hence, noise reduction and vibration suppression in sandwich panels pose major challenges for future aircraft design. Large numbers of references have been devoted to the prediction of the vibroacoustic behavior of such panels. A description and comparison of various analytical methods can be found in Refs. [2-3]. In comparison, there are few published studies on the experimental validation of these models [4]. The objective of this paper is to present the measurement of the various vibroacoustic indicators of two sandwich-composite structures over a large frequency band. The investigated indicators include the structural wavenumber, modal density, damping loss factor, radiation efficiency, and sound transmission loss. For the first four indicators several direct and indirect measurements techniques are presented and compared. Moreover, the measured indicators are also compared to an analytical general laminate model (GLM) [3] and to an equivalent orthotropic panel [4] predictions.

2 DESCRIPTION OF THE MEASUREMENTS

This section describes the measurement of the structural and acoustical properties of the studied panels. They consist of the wavenumber, modal density, damping loss factor, radiation efficiency and the TL. The analysis is performed in a large frequency band starting from 100 Hz to 10 kHz. A comparison between the measured parameters and the presented models are given in Section 3. A thick and a thin flat sandwich-composite panel with a Honeycomb (HC) core construction are studied (Figure 1). They are representative of an aircraft skin and trim panel, respectively. Both panels have a surface area equal to 1.5 m^2 $\left(L_x = 1.5\text{m}, L_y = 1\text{m}\right)$. The thicknesses of the thick and the thin flat panels are 26.4 mm and 6.8 mm, respectively.

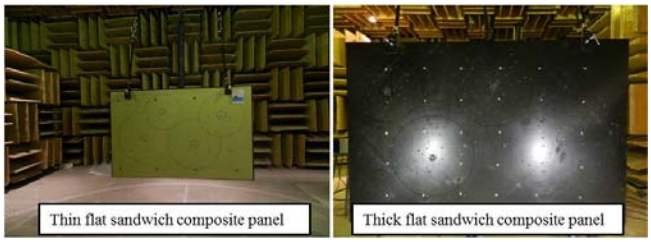

Figure 1. A thin and a thick flat sandwich composite panels.

2.1 Wavenumber measurements

Experimental tests are performed in order to determine the bending wavenumber of the composite plates using both the phase difference [5] and correlation [6] techniques. The phase difference method is based on the measurement of the phase difference φ between accelerometers located at two positions r_1 and r_2 as shown in Figure 2.a.

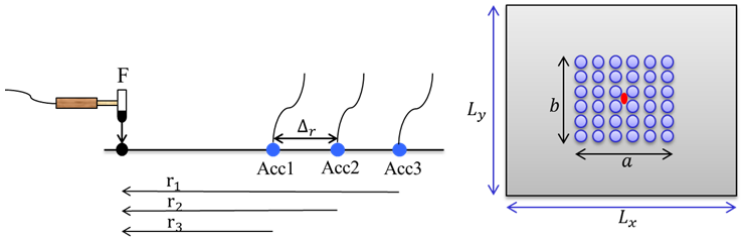

(a) (b)

Figure 2. Measurement setup of: (a) the phase difference technique, (b) the Fourier Transform technique.

The bending wavenumber k_b is given by [5]:

$$\varphi\left(Acc1, Acc2\right) = k_b\left(r_2 - r_1\right). \tag{1}$$

This method assumes the panel flat and of infinite extent and thus doesn't take into account the reflections on the edges of the test panel. The flexural wavenumber was also measured using the correlation technique [5]. This approach is based on the calculation of the two-dimensional space Fourier transform of the surface normal velocity field. For this, the panels were freely hung in a quiet room (semi-anechoic) using flexible chords (Figure 1). A shaker was attached at the centre of the panel through a stringer and was driven by a broadband white noise signal. A scanning laser vibrometer was used to measure the velocity over a surface mesh. The used scan area was 1m by 0.75 m and consisted of 80 points along the X direction and 80 along the Y direction for a total of 6400 measurement points. A schematic is given in Figure 2.b. Measuring the plate normal velocity field, $w\left(x_p, y_q, \omega\right)$, at each point of the scanning area and using the transition to the wavenumber space leads to the flexural wavenumber [6]:

$$\hat{W}\left(k_x, k_y, \omega\right) = \frac{L_x L_y}{N^2}\sum_{p=1}^{N}\sum_{q=1}^{N} w\left(x_p, y_q, \omega\right) e^{-jk_x x_p} e^{-jk_y y_q}. \tag{2}$$

The technique is restricted by the size of the physical scan area, requires equally spaced measurement and is very sensitive to noise in the data. It is still used here to corroborate the results of the classical phase difference method.

2.2 Damping loss factor

The damping loss factor (DLF) of the panels is experimentally derived from the half-power bandwidth method (3dB method), the decay rate method (DRM) and the steady state power input method (PIM). The first technique refers to modal damping which is valid only at low frequency; when possible it is used in the current work as a validation for the other two methods. In the other two methods, the primary property of interest is the band-averaged loss factor. The DRM is based on the logarithmic decrement of the transient structural response, which is obtained from measurement of the decay of accelerometers placed on the structure's surface after the excitation is cut off. Here damping is assumed to follows an exponential decay and all modes in a third-octave band have the same damping. Hence, the damping loss factor is given, for a third-octave band of centre frequency f and slope of the decay DR in units of decibel/second, by the following expression [7]:

$$\eta_i = \frac{DR}{27.3 f}. \tag{3}$$

The third method (PIM) is directly derived from Statistical Energy Analysis (SEA) power balance equation. The damping loss factor is obtained from the measurement of the power supplied to the structure and the spatially averaged square velocity produced. In steady state conditions, the average power input is equal to the average power dissipated and then the average loss factor is [8]:

$$\eta_i = \frac{P_i}{\omega E_i}. \tag{4}$$

2.3 Modal Density

The modal density of the panels is measured with the panel freely suspended inside an anechoic room to minimize radiation coupling between the panel and the room. It is obtained from the measurement of the spatially averaged input mobility following [9]:

$$n(f) = 4MRe(Y_p), \tag{5}$$

where M is the mass of the panel and $Re(Y_p)$ is the real part of the panel's input mobility $Y_p = G_{Fv}/G_{FF}$. G_{Fv} is the cross-spectrum between the force and the velocity signals at the excitation location and G_{FF} is the autospectrum of the force signal. Mass corrections must be considered when making shaker-based frequency response measurement on a lightweight structure because of the added mass coming from the impedance head [10]. In consequence, a corrected admittance Y_c was rather used in Eq.(6). It is obtained using the admittance of the impedance head Y_M , which is measured by exciting the impedance head without the driven plate:

$$Y_c = Y_p \Big/ 1 - \frac{Y_p}{Y_M} \tag{6}$$

The modal densities of the panels were obtained by averaging the modal densities measured at the same four locations used for the measurement of the damping loss factor. The modal densities were also estimated from the measured wavenumbers using [4]:

$$n(\varphi,\omega) = \frac{A_p}{2\pi^2} \frac{k_s(\varphi,\omega)}{\left|c_g(\varphi,\omega)\right|}, \tag{7}$$

where $n(\varphi,\omega)$ is the angular distribution of the modal density and $c_g(\varphi,\omega) = d\omega/dk$ is the group velocity. The results of both measurement methods will be compared to predictions in section 3.

2.4 Radiation efficiency

There are several methods to measure the radiation efficiency of the panels. In this work, an indirect method based on an experimental SEA model of the panel freely hanged in a reverberant room was used. It is obtained by studying energy flow relations between the structure and the reverberation room. The method is based on solving a two subsystems SEA equation where the tested panel is defined as subsystem 1 and the reverberant room as subsystem 2, respectively:

$$\omega\begin{bmatrix} \eta_1+\eta_{12} & -\eta_{21} \\ -\eta_{12} & \eta_2+\eta_{21} \end{bmatrix}\begin{Bmatrix} E_1 \\ E_2 \end{Bmatrix}=\begin{Bmatrix} P_1 \\ P_2 \end{Bmatrix}, \tag{8}$$

where η_{ij} is the coupling loss factor (CLF) between subsystems i and j (with $j \neq i$) and η_i is the damping loss factor of subsystem i.

The radiation efficiency σ is related to the CLF between the tested panel and the reverberant room. Assuming both faces of the panel to radiate equally, $\eta_{12}=2\eta_{rad}$ is thus twice the radiation coupling and in consequence [6]:

$$\sigma=\frac{1}{2}\frac{\omega M}{\rho_0 c_0 A_p}\eta_{12}. \tag{9}$$

In the presented results, the CLF η_{12} is obtained from the inversion of the SEA matrix:

$$\omega\begin{bmatrix} \eta_{11} & -\eta_{21} \\ -\eta_{12} & \eta_{22} \end{bmatrix}=\begin{bmatrix} A_{11} & A_{12} \\ A_{21} & A_{22} \end{bmatrix}^{-1}, \tag{10}$$

where coefficients A_{ij} denote the ratio of the energy (response) of subsystem i to the input power to (excitation of) subsystem j and $\eta_{11}=\eta_1+\eta_{12};\ \eta_{22}=\eta_2+\eta_{21}$. The radiation efficiency of the panel when freely hanged in a semi-anechoic room was also measured for cross validation purposes. It is derived from the measurement of the spatially averaged squared velocity $\langle v^2 \rangle$ and the radiated sound power. The radiation efficiency is defined as the proportionality between radiated sound power P_{rad} and the spatially averaged squared velocity $\langle v^2 \rangle$ over radiation surface A_p:

$$\sigma=\frac{\mathrm{P}_{rad}}{\rho_0 c_0 A_p \langle v^2 \rangle}. \tag{11}$$

2.5 Transmission loss

The TL tests were performed in a semi-anechoic–reverberant transmission loss suite. The measurement follows ISO 15186-1:2000 standard [11]. The panels are clamped in a frame between a reverberant and a semi-anechoic room. White noise was generated in the reverberant room using six loudspeakers and the average sound power is captured using a rotating microphone. On the semi-anechoic side, the sound intensity is measured using an intensity probe with a 6 mm spacer between two 1/4-in microphones. The transmission loss of the structure is given by [4]:

$$TL=L_P-L_i-6. \tag{12}$$

L_P is the average SPL in the source room. L_i is the averaged intensity level over the measurement surface in the receiving room.

3 RESULTS AND DISCUSSION

Comparison between the prediction and experiments are presented and discussed in this section. Damping loss factor, wavenumber, modal densities, and the radiation efficiency are measured for thin and thick composite panels and compared to analytical (general laminate model, equivalent orthotropic panel) predictions.

3.1 Wavenumber

Wavenumber results of the thick and thin composite sandwich panels are shown in Figure 3, respectively. For each panel, the wavenumber curves measured along X and Y directions using the phase difference and correlation techniques are compared. Note that in Figure 3, the acoustic wavenumber (straight line) is also presented to show the acoustic coincidence zone of the panels.

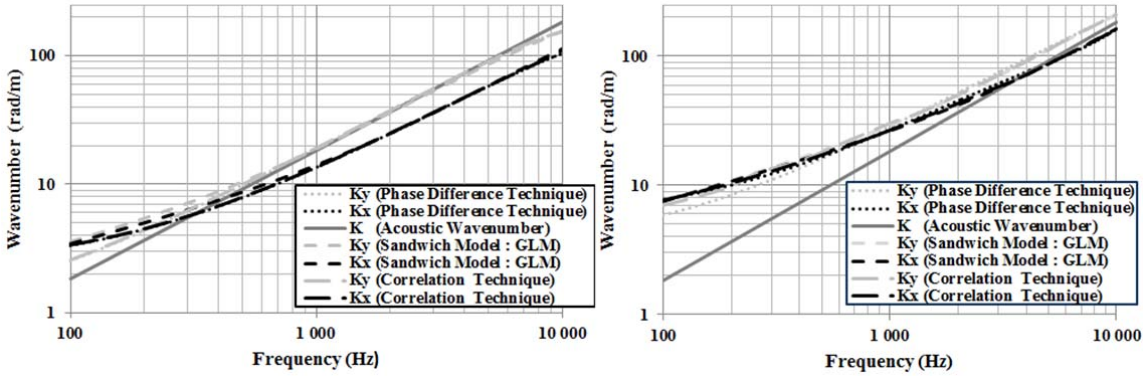

Figure 3. Measured vs. predicted wavenumbers of: (a) the thick panel, (b) the thin sandwich panel.

Overall, the comparisons between the experimental and analytical results are good for both methods. At high frequency, the correlation technique gives a better estimation due to fine mesh used in the scan. However, the method seems less accurate at low frequencies, especially for the thick panel where an overestimation is observed.

3.2 Damping loss factor

Damping loss factor results using the half-power bandwidth method (-3dB), the decay rate method and the power input method are shown in Figure 4. The half-power bandwidth method (-3dB) results are used only as a validation tool when applicable.

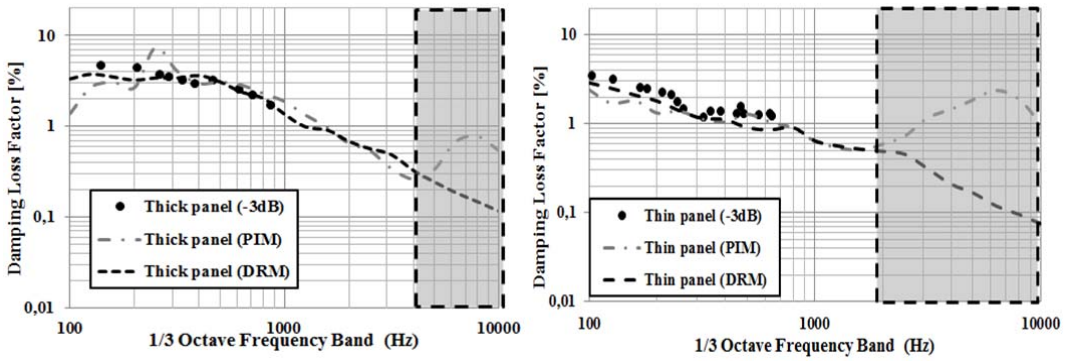

(a) (b)

Figure 4. Measured damping loss factor of: (a) the thick panel, (b) the thin sandwich panel.

For both panels, it is observed that the DRM and the PIM agree well at mid frequencies. However, at low frequency [100–300 Hz], the damping loss factor is better predicted by the DRM compared to the PIM, the reason being the low mode count of the two panels. At high frequency, damping loss factor is also well predicted by the DRM. Meanwhile, the PIM fails (Gray area in Figure 4). The cause was related to an experimental limitation in injecting power into the system in this frequency region. In consequence, in the prediction of the transmission loss, the DRM results will be used.

3.3 Modal Density

Figure 5 shows comparisons of the modal density predicted by the GLM model to measurements (using Eq. (5) for the Input Mobility method and Eq. (7) for the Wavenumber method) for the thick and thin composite sandwich panels, respectively.

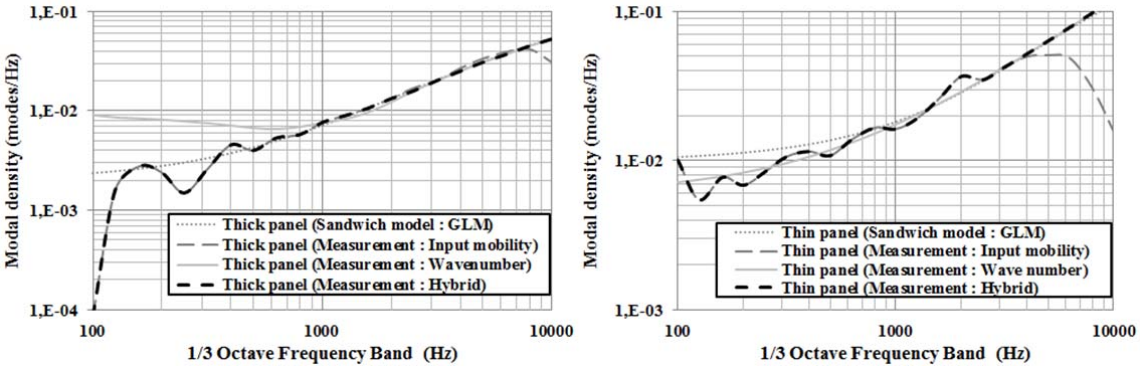

(a) (b)

Figure 5. Measured vs. predicted modal densities of: (a) the thick panel, (b) the thin sandwich panel.

At low and mid frequency, the predicted modal density compares well with measurements using the Input Mobility method for both panels. At higher frequencies, the measurement fails, a consequence again of the difficulty in injecting the power to the panels with the used shaker. On the other hand, good comparison is obtained for both panels at these high frequencies using the wavenumber method. This is logical because a fine scan is used. However, a difference between the measurement and theoretical values are observed at low frequencies, especially for the thick

panel where an overestimation is observed. The cause was related to the previously mentioned limitation in measuring the wavenumber. In consequence, better results are obtained using a Hybrid method which combine the Input Mobility method at low frequency and the Wavenumber method at mid and high frequency (black dotted line in the Figure 5). The Hybrid method results agree well with theory over a large frequency band [200Hz to 10 kHz].

3.4 Radiation efficiency

Fig. 6 shows the comparisons between predictions using the GLM model and measurements for the thick and thin panels, respectively. As discussed before, measurement using both the classical method [Eq.(11)] and experimental SEA [Eq.(9)] were performed and are compared in the two figures.

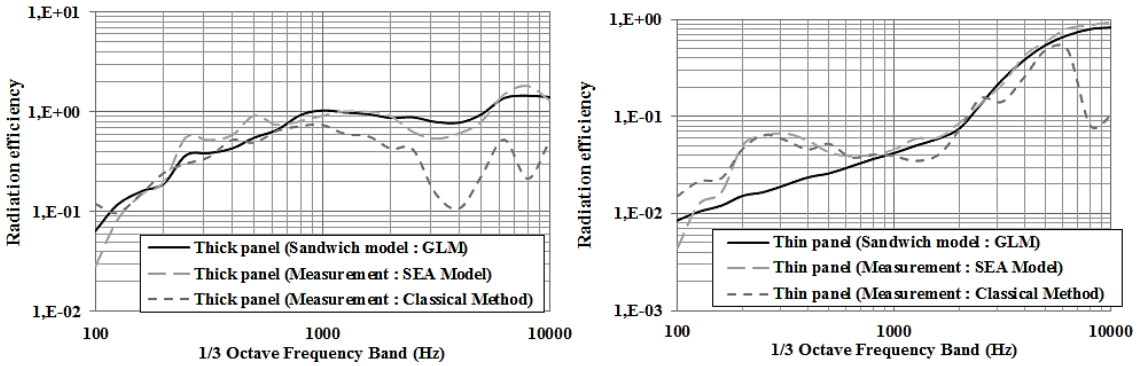

(a) (b)

Figure 6. Measured vs. predicted radiation efficiency of: (a) the thick panel, (b) the thin sandwich panel.

Overall, it is observed that the comparison is fair for both panels between prediction and measurements using the SEA based measurement method. However, the SEA based methodology is limited at low frequencies due to the low mode count. On the other hand, and for both panels, the classical measurement method diverges at high frequencies. The cause was related again to an experimental limitation in injecting power to the system in this frequency region.

3.5 Transmission loss

The comparison between tests and predictions is shown in Figure 7. Two prediction methods are shown. In the first, the surface impedance of the panel calculated using the GLM model is used to estimate the TL. In the second, an equivalent orthotropic panel model is used. For both cases, to account for the damping added by the installation of the panels in the test window, the damping loss factor measured using the decay rate method with the panels mounted in the window was used in the predictions.

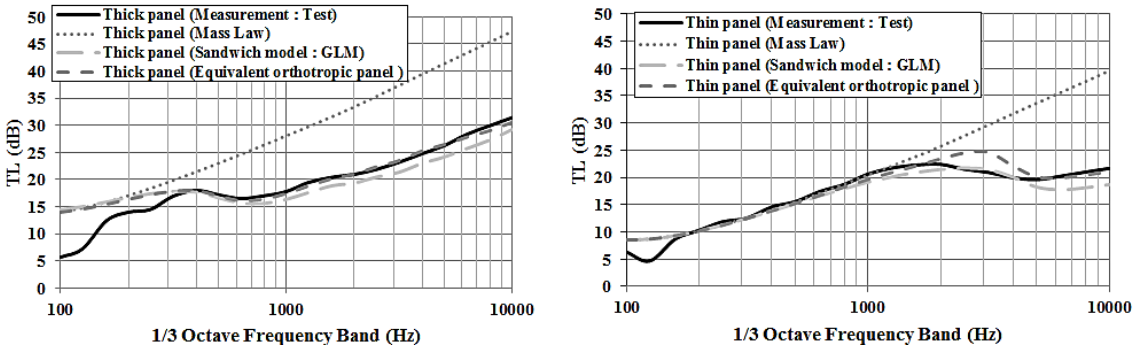

(a) (b)

Figure 7. Measured vs. predicted transmission loss of: (a) the thick panel, (b) the thin sandwich panel.

Figure 7.a shows that the TL prediction of the thick sandwich panel using the equivalent orthotropic panel correlates well with the test results. Predictions using both the measured and predicted wavenumbers leads to the same results. However, the use of the full GLM model underestimates the TL, by approximately 2 dB, starting at the onset of the coincidence region (around 500 Hz). For the thin sandwich panel (Figure 7.b), both models are in good agreement with measurements in the mass-law region. Sandwich model predict well the critical frequency region (around 4000 Hz), while the equivalent panel model overestimates this region. At much high frequencies, the sandwich model tends to underestimate the TL. For this panel, all the above discussed discrepancies are traced to the uncertainties in the measurement of the panel's damping loss factor.

4 CONCLUSION

This paper discusses the measurement of the vibroacoustics indicators of two sandwich-composite structures over a large frequency band. Various experimental methods were used and compared to analytical predictions. It is shown that the GLM model predict very well the wavenumber (dispersion curves), the modal density and the radiation efficiency of the two tested panels. The prediction of the TL while acceptable was however found less satisfactory for the thick panel. The paper also shows that a simple equivalent orthotropic panel model predict with accuracy the transmission loss of the two studied sandwich panels.

ACKNOWLEDGEMENTS

This work was supported by grants-in-aid from the Natural Sciences and Engineering Research Council of Canada (N.S.E.R.C.). Bombardier Aerospace is acknowledged for contributing panels and materials for the tests.

REFERENCES

[1] U. Orrenius. Prediction and control of sound transmission through honeycomb sandwich panels for aircraft fuselage and train floors. 17th International Congress on Sound and Vibration, Cairo, Egypt, 117-124, 2010.

[2] T. Wang, V.S. Sokolinsky, S. Rajaram, and S. Nutt. Assessment of sandwich models for the prediction of sound transmission loss in unidirectional sandwich panels. Applied Acoustics. 66: 245-262, 2005.

[3] S. Ghinet, and N. Atalla. Modeling thick composite laminate and sandwich structures with linear viscoelastic damping. Computers and Structures. 89:1547-1561, 2011.

[4] R. Cherif, and N. Atalla. Experimental investigation of the accuracy of a sandwich model. Journal of the Acoustical Society of America. 137(3):1541, 2015.

[5] J. H. Rindel. Dispersion and absorption of structure-borne sound in acoustically thick plates. Applied Acoustics. 41(2):97-111, 1994.

[6] A. N. Thite, and N. S. Ferguson. Wavenumber Estimation: Further Study of the Correlation Technique and Use of SVD to Improve Propagation Direction Resolution. ISVR Technical Memorandum, 2004.

[7] R. H. Lyon, and R. G. DeJong. Theory and application of statistical energy analysis. Butterworth-Heinemann, Boston, second edition edn, 1995.

[8] D. A. Bies, and S. Hamid. In situ determination of loss and coupling loss factors by the power injection method. Journal of Sound and Vibration. 70(2):187-204, 1980.

[9] B. L. Clarkson. The derivation of modal densities from point impedances. Journal of Sound and Vibration. 77(4):583-588, 1981.

[10] K. Renji, and M. Mahalakshmi. High frequency vibration energy transfer in a system of three plates connected at discrete points using statistical energy analysis. Journal of Sound and Vibration. 296(3):539-553, 2006.

[11] ISO 15186-1:2000. Acoustics – "Measurement of sound insulation in buildings and of building elements using sound intensity" – Part 1: Laboratory measurements. 1-25, 2000.